Anesthesiology 2003; 98:121–32

Ketamine Differentially Blocks Sensory Afferent Synaptic Transmission in Medial Nucleus Tractus Solitarius (mNTS)

Young-Ho Jin, Ph.D. Timothy W. Bailey, Ph.D.,* Mark W. Doyle, Ph.D.,* Bai-yan Li, M.D., Ph.D.,† Kyoung S. K. Chang, M.D., Ph.D.,‡ John H. Schild, Ph.D.,§ David Mendelowitz, Ph.D.,‖ Michael C. Andresen, Ph.D.#*

Background: **Ketamine increases blood pressure and heart rate by unknown mechanisms, but studies suggest that an intact central nervous system and arterial baroreceptors are required. In the brain stem, medial nucleus tractus solitarius receives afferents from nodose neurons that initiate cardiovascular autonomic reflexes. Here, the authors assessed ketamine actions on afferent medial nucleus tractus solitarius synaptic transmission.**

Methods: **Ketamine was applied to horizontally sliced brain stems. Solitary tract (ST) stimulation evoked excitatory postsynaptic currents (eEPSCs) in medial nucleus tractus solitarius neurons. Capsaicin (200 nM) block of ST eEPSCs sorted neurons into sensitive (n = 19) and resistant (n = 23). In nodose ganglion slices, shocks to the peripheral vagal trunk activated afferent action potentials in sensory neurons classified by conduction velocities and capsaicin.**

Results: **Ketamine potently (10–100 μM) blocked small, ST-evoked *N*-methyl-D-aspartate synaptic currents found only in a subset of capsaicin-resistant neurons (6 of 12). Surprisingly, ketamine reversibly inhibited ST eEPSC amplitudes and induced synaptic failure at lower concentrations in capsaicin-sensitive than in capsaicin-resistant neurons ($P < 0.005$; n = 11 and 11). Spontaneous EPSCs using non–*N*-methyl-D-aspartate receptors were insensitive even to 1–3 mM ketamine, suggesting that ST responses were blocked presynaptically. Similarly, ketamine blocked C-type action potential conduction at lower concentrations than A-type nodose sensory neurons.**

Conclusion: **The authors conclude that ketamine inhibits postsynaptic *N*-methyl-D-aspartate receptors and presynaptic afferent processes in medial nucleus tractus solitarius. Unexpectedly, capsaicin-sensitive (C-type), unmyelinated afferents are significantly more susceptible to block than capsaicin-resistant (A-type), myelinated afferents. This differentiation may be related to tetrodotoxin-resistant sodium currents. Since C-type afferents mediate powerful arterial baroreflexes effects, these differential actions may contribute to ketamine-induced cardiovascular dysfunction.**

THE intravenous anesthetic ketamine is generally reported to increase blood pressure and heart rate in humans and experimental animals.[1,2] Among other actions, ketamine alters autonomic nerve activity and baroreflex control.[3] Brain stem sites of action within the central nervous system have been proposed generally,[4,5] although the responsible neurons are unknown. The nucleus tractus solitarius (NTS) is the site of the obligatory first synaptic contacts by critical afferents from the cardiovascular and respiratory system that participate in autonomic reflexes.[6] Microinjection of ketamine into NTS alters baroreflex responses, and this site may contribute to the observed cardiostimulatory effects of ketamine.[7,8] However, the underlying cellular mechanisms of ketamine within NTS are unknown.

Baroreceptor reflexes are initiated within the medial NTS (mNTS) by incoming action potentials conducted along the solitary tract (ST) pathway. The afferent inputs processed in mNTS are then projected to higher-order neurons, including central autonomic efferent neurons.[9] Such afferents include two major classes, those with myelinated, A-type axons and those with unmyelinated, C-type axons. The C-type class is inhibited by capsaicin, a specific ligand for the VR1 receptor present in these neurons.[10,11] Although the functional ramifications of A- and C-type baroreceptor afferents are not entirely clear, activation of C-type baroreceptors elicits larger blood pressure and heart rate changes than A-type baroreceptors at the lowest frequencies of activation.[12,13] In addition, C-type baroreceptors have long been associated with powerful antihypertensive baroreflex responses and regulation of mean blood pressure, while A-type baroreceptors may contribute more to buffering dynamic changes in pressure.[14–16]

Here, we tested whether ketamine alters this afferent synaptic processing at mNTS second-order neurons. We activated ST and recorded synaptic currents with patch electrodes in horizontal slices of rat brain stem. Since these experiments indicated differential presynaptic actions on A- and C-type ST afferents, we also assessed the actions of ketamine on the discharge properties of nodose ganglion sensory neurons. We found that ketamine compromises afferent glutamatergic synaptic transmission by a combination of presynaptic and postsynaptic actions, and, surprisingly, afferent synaptic transmission failed at lower concentrations of ketamine in capsaicin-sensitive neurons than in capsaicin-resistant neurons. Thus, ketamine differentially alters afferent synaptic transmission within mNTS and as such has the potential for producing the sorts of differential autonomic effects (sympathetic–parasympathetic and cardiac–peripheral resistance) often observed and attributed to brain stem mechanisms.[4,17,18]

* Postdoctoral Fellow, # Professor, Department of Physiology and Pharmacology, Oregon Health & Science University. † Senior Scientist, § Assistant Professor, Biomedical Engineering Program, Indiana University–Purdue University, Indianapolis, Indiana. ‡ Associate Professor, Department of Anesthesiology, Oregon Health & Science University and Veterans Affairs Medical Center, Portland, Oregon. ‖ Associate Professor, Department of Pharmacology, George Washington University, Washington, DC.

Received from the Department of Physiology and Pharmacology, Oregon Health & Science University, Portland, Oregon. Submitted for publication May 10, 2002. Accepted for publication August 20, 2002. Supported in part by grant No. R01 HL-58769 from the U.S. National Institutes of Health, Bethesda, Maryland.

Address reprint requests to Dr. Andresen: Department of Physiology and Pharmacology, Oregon Health & Science University, Portland, Oregon 97201-3098. Address electronic mail to: andresen@OHSU.edu.

Materials and Methods

All animal procedures were performed with the approval of the Institutional Animal Care and Use Committee at Oregon Health & Science University (Portland, Oregon) or Indiana University–Purdue University (Indianapolis, Indiana) and are in accordance with the recommendations of the Panel on Euthanasia of the American Veterinary Medical Association and the National Institutes of Health publication "Guide for the Care and Use of Laboratory Animals."

Slice Preparation

Brain stem slices were prepared from adult (100–300 g) male Sprague-Dawley rats (Charles River Laboratories, Inc., Wilmington, MA). Rats were briefly anesthetized with halothane and quickly killed by cervical dislocation. These methods were identical to those previously described in detail.[19] Briefly, the medulla was removed and trimmed rostrally and caudally to yield a 1-cm block centered on the obex. The ventral surface of the block of brain tissue was cut so as to reorient the plane of blade travel to cut 250-μm slices that contained lengthy segments of the ST together with mNTS neurons. Slices were cut with a sapphire knife (Delaware Diamond Knives, Wilmington, DE) mounted in a vibrating microtome (VT1000S; Leica Microsystems Inc., Bannockburn, IL). The external solution was an artificial cerebrospinal fluid (ACSF) containing the following: 125 mM NaCl, 3 mM KCl, 1.2 mM KH_2PO_4, 1.2 mM $MgSO_4$, 25 mM $NaHCO_3$, 10 mM dextrose, and 2 mM $CaCl_2$, bubbled with 95% O_2–5% CO_2. Slices were secured with a nylon mesh in a custom perfusion chamber and perfused with ACSF at 32–35°C, 307 mOsm, bubbled with 95% O_2–5% CO_2. Recordings were made from mNTS neurons located just medial to the ST and within 200 μm rostral or caudal from the obex, the area of densest aortic baroreceptor afferent terminations.[19,20]

Visualized Patch Recordings

Neurons were visualized with differential interference contrast optics (40× water immersion lens) using an Axioskop 2 microscope (Zeiss, Thornwood, NJ) and an infrared-sensitive camera. Patch electrodes were guided using infrared differential interference contrast microscopy to neurons. Voltage clamp was performed in the ruptured, whole cell configuration (Axopatch 200A; Axon Instruments, Foster City, CA). Recording electrodes (2.5–3.5 MΩ) were filled with an intracellular solution containing the following: 10 mM NaCl, 130 mM K Gluconate, 11 mM EGTA, 1 mM $CaCl_2$, 2 mM $MgCl_2$, 10 mM N-2-hydroxyethylpiperazine-N'-2-ethanesulfonic acid (HEPES), 2 mM Na_2ATP, and 0.2 mM Na_2GTP; pH 7.3; 295 mOsm. Data were filtered at 3 kHz and sampled at 50–10 kHz using p-Clamp8 software (Axon Instruments). Stimuli were delivered *via* a concentric bipolar stimulating electrode (200-μm diameter; Frederick Haer Co., Bowdoinham, ME) placed on the visible ST. Since the stimulation electrode was placed 1–3 mm from the site of the recorded neuron soma, we minimized the possibility of focal stimulation of non-ST axons or local cell bodies. Bursts of five ST stimuli every 3 s (stimulation duration 0.1 ms) at frequencies of 50 or 100 Hz were generated with a Master-8 isolated programmable stimulator (A.M.P.I., Jerusalem, Israel) and evoked excitatory postsynaptic currents (eEPSCs). Synaptic latencies were measured as the time between the onset of the stimulus artifact and the onset of synaptic current. For improved precision, membrane current traces were first differentiated, and these two onset times were taken as crossing points of a set threshold level.[19] The absence of a synaptic current deflection following a stimulus shock to the ST was taken as a synaptic failure, and the rate of failure was calculated as the number of failed synaptic responses to bursts of stimuli (> 50 Hz) across multiple trials. The failure rate was calculated as the number of absent synaptic responses divided by the number of stimulus shocks delivered and expressed as a percentage. Following recording of control synaptic responses, the bath perfusate was changed to a ketamine containing ACSF, and synaptic transmission reassessed at progressively increasing concentrations until synaptic transmission failed. Synaptic transmission was recovered in all cases of perfusion in ketamine-free solution.

Differentiation of Solitary Tract Afferent Subtype

Following completion of each mNTS ketamine protocol, ST synaptic transmission was restored by perfusion in ketamine-free solution and then tested for capsaicin sensitivity in all neurons. Cranial visceral afferent nerves, such as the aortic depressor nerve, contain a slowly conducting C-type class of afferent axon that is blocked by capsaicin (capsaicin-sensitive) and a rapidly conducting A-type class of lightly myelinated afferents that are capsaicin resistant.[12] Both classes of afferent neurons send fibers through the ST to innervate second-order mNTS neurons, and capsaicin-sensitive ST EPSCs can be blocked with sustained capsaicin.[11] At the end of each of the mNTS experiments, 200 nM capsaicin was added to the perfusate to test for capsaicin sensitivity. Capsaicin completely blocked ST synaptic transmission to capsaicin-sensitive second-order mNTS neurons within 10 min. Capsaicin-resistant neurons were unaffected by this capsaicin test. No intermediate responses—partial blockade of EPSCs—were observed. Note that all synaptic and ketamine testing was performed prior to testing for capsaicin sensitivity since the time course of recovery from capsaicin was quite long (> 45 min).[11]

Nodose Neuron Slice Experiments

The nodose ganglion contains the cell bodies of the afferent neurons sending processes *via* the ST to mNTS.

Nodose neuron recordings were performed using enzymatically treated slices of nodose ganglia from adult (250–400 g) Sprague-Dawley rats of either gender (Harlan, Indianapolis, IN). The details regarding the surgical procedure and tissue preparation are described in detail elsewhere.[21] Briefly, in deeply anesthetized rats (methoxyflurane; Schering-Plough Animal Health Corp., Union, NJ), we exposed the vagus nerve from the jugular foramen for a length of 2 cm caudally. The vagus nerve was carefully freed from surrounding tissue. The vagus nerve and attached ganglion were immediately placed into a Petri dish containing chilled (4–8°C) recording solution (see Nodose Recording Solutions). This procedure was performed bilaterally. Microdissection in the dish gently removed excess connective tissues. The bulb of the nodose ganglion was opened using a microdissection scalpel or a vibrating microtome (VT1000S). The microtome provided better control over the angle and orientation of the cut with respect to the vagus nerve. The ganglia-nerve preparation was incubated for 40 min at 37°C in a Ca^{+2}- and Mg^{+2}-free solution of Earle's balanced salt solution (Sigma-Aldrich Corp., St. Louis, MO) with type II collagenase (1 mg/ml at 358 U/mg; Worthington Biochemical Corp., Lakewood, NJ). This solution was then exchanged for one containing Trypsin-3X (4 mg/ml at 181 U/mg; Worthington Biochemical Corp.) and was returned to the incubator for 15 min. The ganglia were then repeatedly washed using chilled (4–8°C), enzyme-free recording solution and were allowed to recover for approximately 30 min prior transferring to the recording chamber.

Nodose Recording Solutions

The bathing solution for current clamp recordings at physiologic temperatures (35–36°C) consisted of the following: 112 mM NaCl, 4.2 mM KCl, 2 mM $CaCl_2$, 1 mM $MgCl_2$, 1.2 mM KH_2PO_4, 25 mM $NaHCO_3$, and 10 mM dextrose, bubbled with 95% O_2–5% CO_2. For recordings at room temperatures (21–23°C), the extracellular medium consisted of the following: 137 mM NaCl, 5.4 mM KCl, 1 mM $MgCl_2$, 2 mM $CaCl_2$, 10 mM glucose, and 10 mM HEPES, with the pH adjusted to 7.3 using 1 N NaOH. The flow rate through the recording chamber was approximately 2 ml/min, and complete exchange occurred in less than 1 min. The pipette solution contained the following: 4 mM NaCl, 50 mM KCl, 50 mM K_2SO_4, 5 mM $MgCl_2$, and 10 mM HEPES. The pH was adjusted to 7.2 using 1 N KOH. Just prior to recording, 2 mM each of Na-GTP and Na-ATP were added to the pipette solution along with 0.25 mM $CaCl_2$ and 4 mM 1,2-bis (2-aminophenoxy) ethane-N,N,N',N'-tetra acetic acid tetra potassium salt (Bapta-K; Sigma-Aldrich Corp.) for a final buffered $[Ca^{+2}]_i$ of 10 nM. During all experiments, the pipette-filling syringe was kept chilled (8–12°C) and isolated from light.

Nodose Ganglion Electrophysiological Techniques

All recordings were conducted using the ruptured patch technique and an Axoclamp-2B amplifier (Axon Instruments) operating in bridge mode as previously described.[21] Glass pipettes were pulled and fire polished to a resistance of 1–1.5 MΩ. Following the formation of a gigaohm seal, the pipette capacitance was compensated. Upon going whole cell, the bridge was balanced to compensate for the electrode access resistance. Two stimulus protocols were utilized: brief ($\geq$ 500 μs), constant current pulses ($\leq$ 400 pA) delivered through the patch electrode and short-duration ($\geq$ 200 μs), monophasic, constant current pulses applied to the vagus nerve using a platinum (90%)-iridium (10%) bipolar electrode with the cathode positioned a measured distance (~1–1.5 cm) from the center of the nodose ganglion. An interelectrode spacing of 2 mm kept the stimulus artifact to less than 0.5 ms in duration. As a result, conduction velocities as high as 20 m/s could easily be resolved with a 1.5-cm length of nerve. The stimulus magnitude was dependent upon the axonal fiber type and was increased approximately 20% beyond the activation threshold just prior to recording. All data were low pass filtered to 10 KHz and digitized at 40 KHz. The experimental protocols and data collection were carried out using the Digidata 1322A under the control of pCLAMP 8 (Axon Instruments).

Drugs

In all experiments, ketamine was applied *via* inclusion in the bath perfusate. Other drugs were similarly applied in conjunction with ketamine as described in the Results. Capsaicin, D-AP5, ketamine, NBQX, and all other drugs were purchased from RBI-Sigma-Aldrich Corp. (St. Louis, MO). Capsaicin was dissolved in ethanol (1 mM) as stock solution, and then the stock solution was diluted with external solution just before use. The final concentration of ethanol was always less than 0.02%. At these concentrations, ethanol alone had no effect on membrane properties (holding current or resistance, data not shown). Ketamine was directly dissolved in ACSF just before use. All the drugs were bath applied for a minimum of 5 min at each concentration and were delivered in order of increasing concentrations. This was sufficient time for all responses to reach a stable value.

Data Analysis of Nodose Action Potentials

To differentiate particular features of the action potentials (APs) evoked across A- and C-type neurons, a standard set of measurements were made on each waveform: AP peak height (AP_{Peak}), peak afterhyperpolarization (AHP_{Peak}), AP duration as measured at one half the displacement between the AP_{Peak} and AHP_{Peak} (APD_{50}), time required for the membrane voltage to return within 20% of the resting membrane potential following an AP (*i.e.*, time to dissipate 80% of the AHP, AHP_{80}), upstroke

velocity as measured at APD_{50} (UV_{APD50}), maximum upstroke velocity (UV_{MAX}), downstroke velocity as measured at APD_{50} (DV_{APD50}), and maximum downstroke velocity (DV_{MAX}). Conduction velocity was calculated as the ratio of the distance between the cathode of the stimulus electrode and the center of the ganglion, and the transit time between the stimulus artifact and the AP threshold. These parameters were used to assess the changes in action potential characteristics during ketamine.

Statistical Analysis

All data are expressed as mean ± SD. IC_{50} values were estimated from curve fits to sigmoidal relations using a nonlinear curve-fitting routine (Origin 6.1; Origin Lab Corp., Northampton, MA). To evaluate differences, parameter values were compared by repeated-measures analysis of variance (ANOVA) or one-way ANOVA (as appropriate) for the effects of treatments (*e.g.*, ketamine) or groups (capsaicin resistant/sensitive). *Post hoc* comparisons of means used the Bonferroni correction for multiple comparisons where appropriate (Statview 4.57; Abacus Concepts, SAS Campus Drive, Cary, NC). In addition, in some cases, the *t* test was used to discern significant differences after interventions. For nodose studies, all averaged data were presented as mean ± SD, and a paired Student *t* test was used to assess the difference in mean values. Differences were considered statistically significant at *P* values of less than 0.05. For clarity, some data sets are presented as values normalized to control (see individual figures), although all statistical testing was performed without normalization.

Results

Capsaicin-sensitive and Capsaicin-resistant mNTS Neurons

Intermittent bursts of high-frequency stimuli (50–100 Hz) delivered to the ST evoked bursts of eEPSCs (evoked excitatory postsynaptic currents) in mNTS neurons (fig. 1). Successive eEPSCs within these burst responses had a pronounced frequency-dependent depression that is characteristic of second-order mNTS neurons.[19,22] These neurons were divided into capsaicin sensitive (n = 19) and capsaicin resistant (n = 23), depending on whether their ST eEPSCs were blocked by 10 min of exposure to capsaicin (200 nM). Capsaicin significantly reduced eEPSC amplitude in capsaicin-sensitive neurons (n = 9; fig. 1A, right; fig. 2A; RM ANOVA, $P < 0.0001$), whereas eEPCSs in capsaicin-resistant neurons were unaffected (n = 10; fig. 1B, right; fig. 2A; RM ANOVA, $P = 0.33$). Coincident with reduction in eEPSC amplitude, capsaicin also increased the holding current (fig. 1A, right; fig. 2B; RM ANOVA, $P = 0.0004$) in capsaicin-sensitive neurons. Similar treatment of capsaicin-resistant neurons failed to alter the holding current

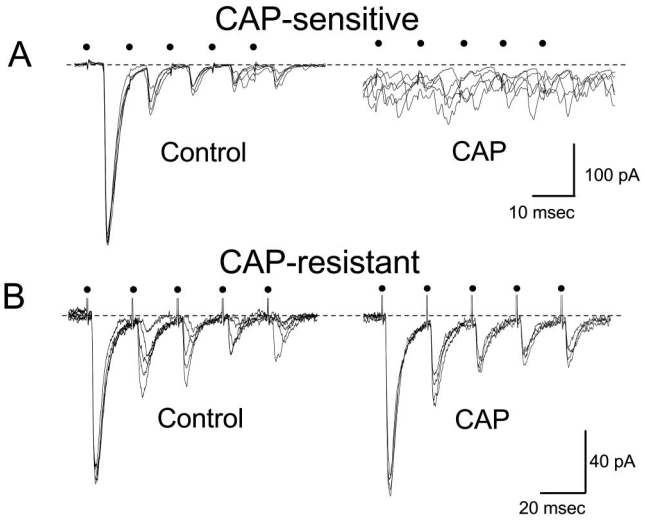

Fig. 1. Two classes of medial NTS neurons were identified based on blockade of afferent synaptic transmission by capsaicin (CAP). Solitary tract (ST) shocks (filled circles) reliably, and at nearly invariant latency, activated evoked excitatory postsynaptic currents (eEPSCs). Each panel shows five consecutive, unaveraged eEPSC traces for responses to trains of five ST stimuli (100 Hz) in these two representative neurons (*A* and *B*). The horizontal broken line represents the mean level of the holding current before capsaicin treatment at a V_H of −70 mV. (*A*) In capsaicin-sensitive neurons, ST eEPSCs were blocked following 5 min in 200 nM capsaicin. After capsaicin (*A, right*) these neurons showed increased spontaneous EPSCs not aligned with ST stimuli. (*B*) In capsaicin-resistant neurons, eEPSC responses were unaltered after 5 min of capsaicin (200 nM) treatment.

(fig. 2B; RM ANOVA, $P = 0.767$). The average latency for eEPSCs was significantly longer in capsaicin-sensitive neurons compared to capsaicin-resistant neurons (fig. 2C; unpaired *t* test, $P = 0.011$). This, at least in part, likely reflects the slower action potential conduction

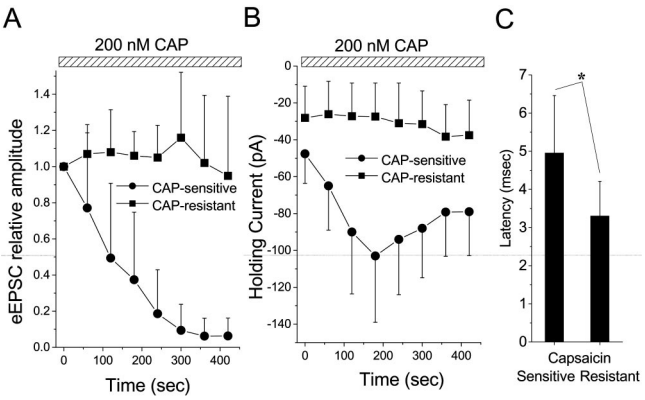

Fig. 2. Summary of average effects of capsaicin (CAP; horizontal bars) on solitary tract (ST) evoked excitatory postsynaptic current (eEPSC) amplitude (*A*, normalized to control, 1.0) and holding currents (*B*) for capsaicin-sensitive (circles, n = 10) and capsaicin-resistant (squares, n = 9) cells. Capsaicin, 200 nM, blocked eEPSCs in capsaicin-sensitive but did not alter those in capsaicin-resistant cells. Holding current increased in capsaicin-sensitive but not in capsaicin-resistant neurons. Points and bars are mean ± SD. (*C*) *Mean of EPSC latencies for capsaicin-sensitive neurons (n = 19) was significantly greater ($P = 0.011$) than for capsaicin-resistant (n = 23).

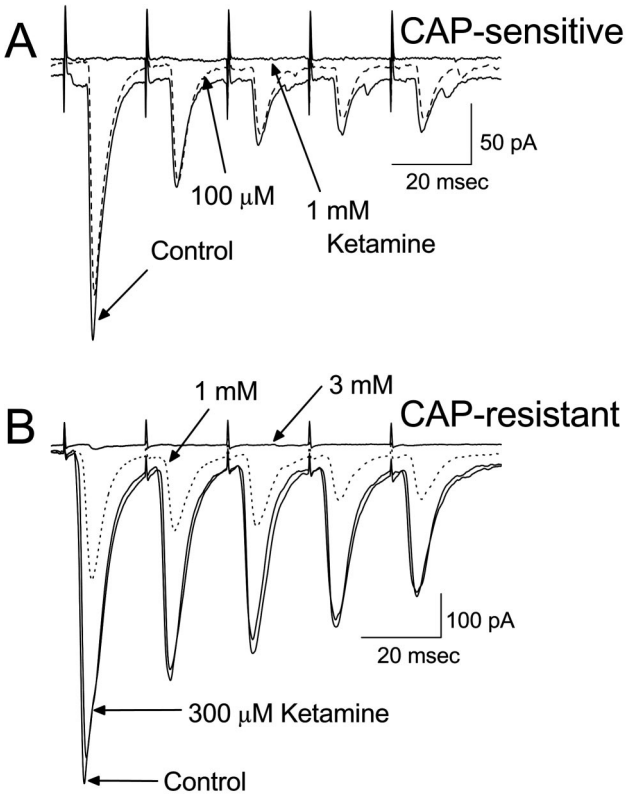

Fig. 3. Ketamine depression of evoked excitatory postsynaptic currents (eEPSCs) in representative capsaicin (CAP)-sensitive and capsaicin-resistant medial NTS neurons ($V_H = -70$ mV). (*A*) Ketamine, 1 mM, completely blocked eEPSCs within 5 min in this capsaicin-sensitive neuron. (*B*) In a capsaicin-resistant neuron, 3 but not 1 mM ketamine completely blocked eEPSCs. Each trace is a mean representing the average of 10 consecutive, individual eEPSC traces at each condition.

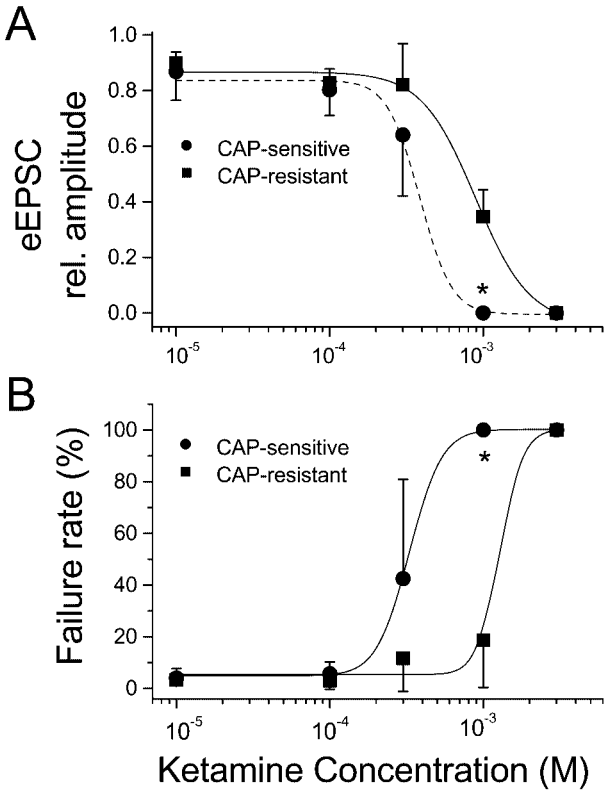

Fig. 4. Summary concentration–response relations for ketamine effects on evoked excitatory postsynaptic current (eEPSC) amplitude and failure rate for capsaicin (CAP)-sensitive (n = 11, circles) and capsaicin-resistant (n = 11, squares) medial NTS neurons. (*A*) Ketamine decreased the amplitude of eEPSCs in capsaicin-sensitive cells at significantly lower concentrations than capsaicin-resistant cells. An IC_{50} value was estimated from a curve fit of to each set of measured data values using sigmoidal logistic relations (capsaicin-sensitive IC_{50} = 386 μM, broken lines; capsaicin-resistant IC_{50} = 1,111 μM, solid lines). Relations are displayed as solid lines for capsaicin resistant ($\chi^2 = 2.09 \times 10^{-3}$) and broken lines for capsaicin sensitive ($\chi^2 = 4.62 \times 10^{-33}$). (*B*) Ketamine increased the synaptic failure rates of eEPSCs. Ketamine blocked eEPSCs at lower concentrations in capsaicin-sensitive cells than in capsaicin-resistant cells. An IC_{50} value was estimated as capsaicin-sensitive IC_{50} = 329 μM and capsaicin-resistant IC_{50} = 1,280 μM. Relations are displayed as solid lines for capsaicin resistant ($\chi^2 = 0.693$) and broken lines for capsaicin sensitive ($\chi^2 = 17.8$). Points and bars are mean ± SD. *Significant differences between capsaicin sensitive and capsaicin resistant at single ketamine concentrations.

velocity in the VR1 containing unmyelinated C fibers than myelinated A fibers. Thus, capsaicin treatment identifies two populations of second-order mNTS neurons.

Ketamine Responses Differ by mNTS Afferent Subtype

Ketamine depressed and then at the highest concentrations completely eliminated ST eEPSCs in both capsaicin-sensitive and capsaicin-resistant neurons (fig. 3). The concentration–response relation was particularly steep in individual neurons, and raising the ketamine concentration resulted in complete disappearance (*i.e.*, failure) of the eEPSC, often without an observed depression in amplitude. Such failures of eEPSCs increased the variance of mean values across group averages. Ketamine at reduced eEPSC amplitudes at significantly lower concentrations in capsaicin-sensitive than capsaicin-resistant neurons (fig. 4A; $P = 0.0053$) by one-way ANOVA and the Bonferroni *post hoc* test. Likewise, synaptic failures appeared at lower concentrations in capsaicin-sensitive neurons (fig. 4B; $P = 0.0006$). Ketamine block of eEPSCs could potentially arise from presynaptic or postsynaptic mechanisms or a combination.

Interestingly, very high concentrations of ketamine (up to 3 mM) failed to eliminate spontaneous, non–*N*-methyl-D-aspartate (NMDA) synaptic transmission while selectively blocking the response evoked by ST stimulation (fig. 5). In both capsaicin-sensitive and capsaicin-resistant neurons, spontaneous EPSCs (sEPSCs) were recorded simultaneously with ST eEPSCs under control conditions (fig. 5A). While 1–3 mM ketamine eliminated ST eEPSCs, the sEPSCs remained in these same neurons at these concentrations (fig. 5B). Nonetheless, like most ST eEPSCs, all sEPSCs that remaining during ketamine were completely blocked by NBQX (fig. 5C) and thus utilized non-NMDA receptors.[19,22] Such observations

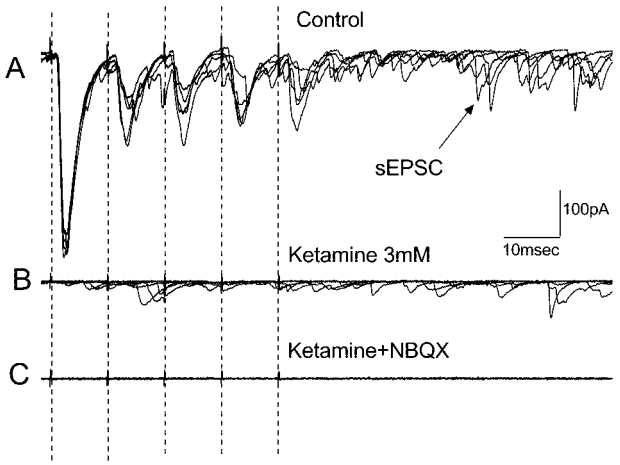

Fig. 5. Afferent-evoked and spontaneous evoked excitatory postsynaptic currents (EPSCs) are differentially ketamine sensitive in medial NTS neurons. Solitary tract stimulation (broken vertical lines) evoked eEPSCs that were eliminated by 3 mM ketamine. Note numerous spontaneous EPSCs (sEPSCs) especially following the end of stimulation (right, *A* and *B*). Ketamine, 3 mM, did not eliminate sEPSCs (*B*). NBQX, 20 μM, blocked the remaining sEPSCs (*C*). Each panel superimposes five unaveraged, consecutive traces.

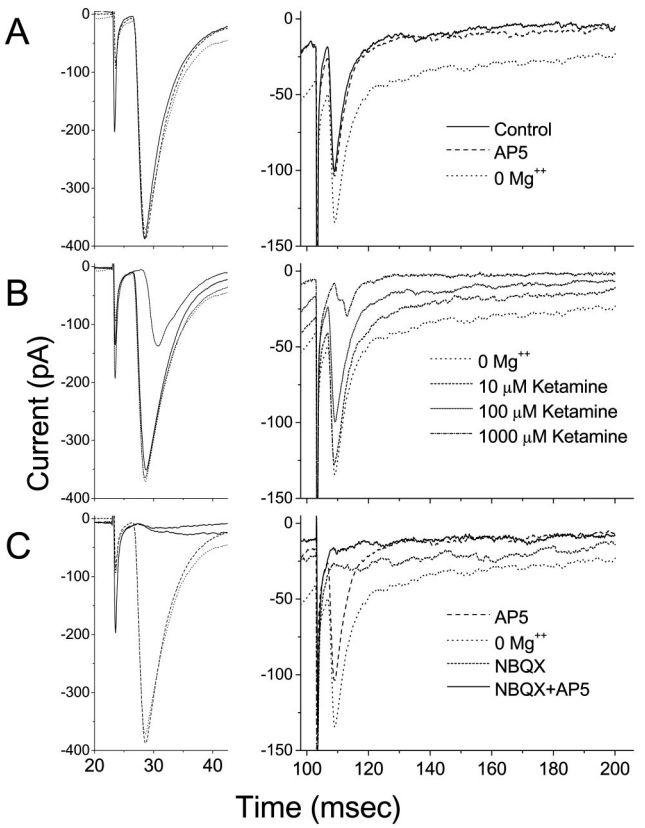

Fig. 6. *N*-methyl-D-aspartate (NMDA) receptor component of solitary tract (ST) synaptic transmission of some capsaicin-resistant medial NTS neurons. In a representative neuron, ST activation evoked a synaptic current (I_{NMDA}) that ketamine potently inhibited. Slowly developing inward synaptic currents were observed in a subset of capsaicin-resistant neurons, and this component increased in zero-Mg external solutions (*A*). The selective NMDA receptor antagonist AP5 (100 μM) reversibly blocked these slow currents (*A*). The synaptic I_{NMDA} was inhibited by 10–100 μM ketamine with only modest effects on the fast, non–NMDA-mediated components (*B*). The fast component of evoked excitatory postsynaptic current (eEPSC) was blocked by NBQX (20 μM), and the slower component was blocked by AP5 (*C*). NBQX in combination with AP5 blocked the entire synaptic current. All effects were reversible on washing. Responses displayed are to a train of five ST shocks, with only the initial EPSC (to the first shock of the train) displayed to the left and the last EPSC (to the fifth shock of the train) displayed to the right. Note that the responses to the fifth shock are plotted on a greatly amplified y-axis compared to the first shock responses. Each current trace represents the averaged current of 11 consecutive traces. All traces were recorded from the same cell.

strongly suggest that ketamine selectively blocked afferent eEPSCs through a presynaptic mechanism and that the site of action is unique to the peripheral afferent nerve process. Thus, the difference in ketamine responses between capsaicin-sensitive and capsaicin-resistant neurons likely reflects a difference between the presynaptic axon or synaptic terminals contacting these capsaicin-sensitive and capsaicin-resistant mNTS neurons.

Ketamine Block of NMDA Component in Subset of mNTS Neurons

Ketamine noncompetitively blocks responses to externally applied NMDA in dissociated NTS neurons[23] and the cardiovascular responses to NMDA microinjected into mNTS.[7,8] In a subset of our capsaicin-resistant neurons, the ST eEPSCs developed a noticeable plateau of steady current during the bursts of five ST shocks, and this steady current decayed slowly following stimulation (fig. 6). Such responses resemble activation of NMDA receptors found in many central nervous system neurons but are uncommon in mNTS.[19,22] To remove voltage-dependent block by Mg^{2+} and better reveal NMDA receptor–mediated currents at holding potentials near rest (V_H = −70 mV), the normal external solution was replaced with ACSF containing no added Mg^{2+} (fig. 6A). In 0 Mg^{2+}, the slowly developing inward synaptic currents increased in amplitude, and the eEPSC amplitude increased. This slow current component was reversibly blocked by 100 μM AP5, a selective NMDA receptor antagonist (fig. 6A). Interestingly, the NMDA component was observed in only 6 of 12 capsaicin-resistant neurons. All tested capsaicin-sensitive neurons had no NMDA component under these conditions (n = 7). Ketamine, 10 μM, attenuated and 100 μM ketamine completely blocked this NMDA component without significantly affecting the fast, non-NMDA component (fig. 6B). Ketamine, 1,000 μM, delayed and severely attenuated the rapid, non-NMDA (NBQX-sensitive) component as well (fig. 6B). NBQX blocked the rapid portion of the eEPSC, leaving a slowly developing, slowly dissipating inward current (fig. 6C, left and right, respectively). The combination of NBQX (20 μM) and AP5 (100 μM) completely blocked the eEPSCs. All ketamine effects on NMDA com-

ponents were rapidly reversed upon washing in ketamine-free solutions.

Ketamine Actions in Nodose Afferent Neurons

The mNTS slice studies strongly suggested that the mechanism for blockade of eEPSCs by ketamine was dependent on the properties of the ST presynaptic axon type. The nodose ganglion contains the cell bodies of the majority of the afferent axons in the ST.[6] Thus, we examined the discharge properties of A- and C-type nodose neurons to try to assess their ketamine sensitivity. Action potentials could be evoked in nodose neurons by constant current shocks to the peripheral vagal trunk (fig. 7), and such axonal shocks activate responses that conducted into the recorded neuronal cell body. Alternatively, direct intracellular current injection through the patch recording electrode could directly activate a somatic action potential (fig. 8). Action potentials were constant in their characteristics over times equivalent to the longest experiments (30 min).[21] In individual neurons, both the action potential wave shape and the conduction velocity were characteristic of either A-type myelinated or C-type afferents (fig. 7). At physiologic temperatures, 100 μM ketamine rapidly slowed the conduction velocity and broadened the action potentials of C-type afferents by 3 min of exposure (fig. 7A). Over this time course, significant changes in the AP wave shape could be broadly described as a reduction in the overall excitability of the neuron. Ketamine (100 μM) altered nearly every recorded measure of the action potential wave shape and conduction velocity of C-type sensory afferents (table 1). Comparable changes occurred at room temperature (fig. 7B). Longer perfusion times eventually led to complete failure of conduction in this C-fiber afferent. In contrast, A-type afferents showed no significant changes in conduction velocity or action potential wave shape after 3 min of perfusion with 100 μM ketamine (fig. 7C). Reductions in conduction velocity and changes in action potential wave shape did occur with perfusion times greater than 10 min, but it could not be determined whether these changes were due to ketamine or to technical difficulties associated with maintaining gigaohm seals on A-type neurons patched in the ganglion slice.[21]

Somatic APs could also be directly evoked by current injection through the recording electrode (fig. 8). Action potentials conducted to the soma after vagal trunk stimulation failed during ketamine exposure several minutes before somatic current injection failed to evoke a direct somatic AP (fig. 8). This suggests that the axonal conduction process failed before action potential generation *per se*. These directly evoked somatic action potentials in C- and A-type nodose neurons were also differentially sensitive to ketamine (fig. 8). Within 1 min of 100-μM ketamine exposure, the action potential wave shape was transformed. Nearly all measures of the action potential

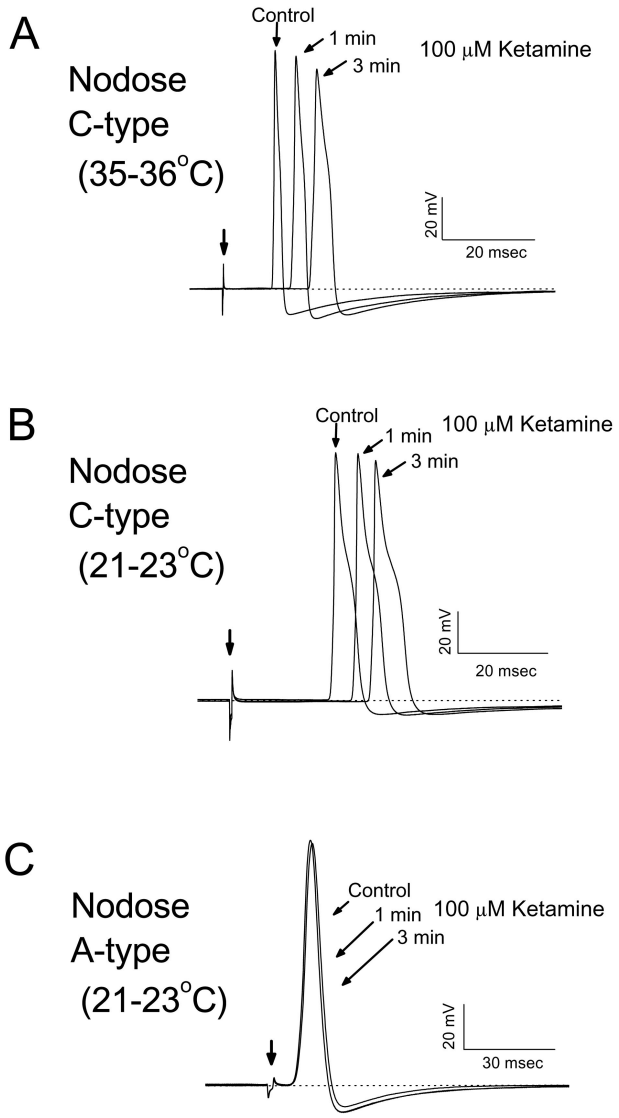

Fig. 7. Effects of 100 μM ketamine upon nerve-evoked somatic action potentials of C- and A-type neurons. Time course of ketamine effects at physiologic temperatures (35–36°C) upon a C-type afferent fiber (conduction velocity, 1.4 m/s) (*A*), at room temperatures (21–23°C) upon a C-type afferent fiber with a conduction velocity of 0.7 m/s (*B*), and at room temperatures upon an A-type afferent fiber with a conduction velocity of 15 m/s (*C*). Within the first few minutes of ketamine perfusion, the conduction velocity of all C-type afferents slowed dramatically as indicated by the progressively later arrival of action potentials. Furthermore, action potential waveforms broadened substantially (*A* and *B*). In contrast, the conduction velocity and waveshape of all A-type afferents were unaffected by the same concentration of ketamine. All voltage recordings were made from a membrane potential adjusted to −60 mV (dashed line) *via* continuous direct current injection through the recording electrode. Monophasic constant current pulses (≥ 500 μs) of fixed magnitude were applied to the vagus nerve using a bipolar electrode positioned a known distance from the center of the ganglion (horizontal dashed line).

wave shape in C-type neurons changed substantially during ketamine, with the exception of AHP_{Peak} and AHP_{80} (table 1). As with the nerve trunk evoked conducted action potentials, A-type somatic action potentials were

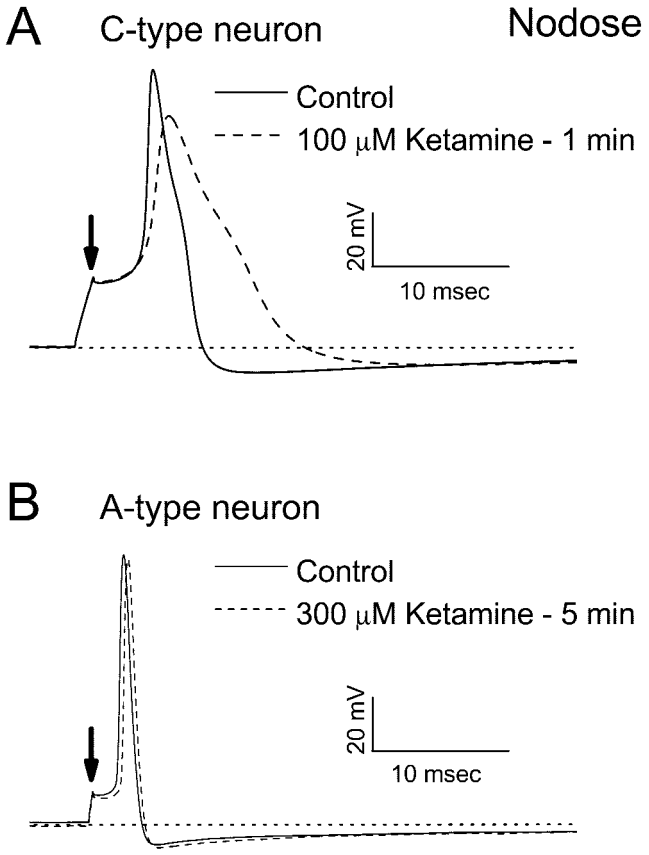

Fig. 8. Effects of ketamine perfusion at room temperatures (21–23°C) upon somatic action potentials from representative C-type (0.7 m/s, *A*, 100 μM) and A-type (14.2 m/s, *B*, 300 μM) nodose neurons within the intact ganglia. The action potential waveshape of C-type neurons was reduced and broadened almost immediately upon ketamine perfusion, while that of A-type cells was unchanged following 5 min of ketamine perfusion. For all recordings, monophasic constant current pulses (< 500 μs) of fixed magnitude were applied through the patch recording electrode (arrow) from a membrane potential adjusted to −60 mV (dashed line) *via* continuous direct current injection through the recording electrode.

essentially unaffected by ketamine concentrations as high as 300 μM and for perfusions as long as 5 min.

Our testing paradigm consisted of three supramaximal shocks to the vagus nerve delivered at 1 Hz. Over the first several minutes of ketamine exposure, conduction slowed, the action potential appeared later after each shock, and the action potential progressively broadened (fig. 9A). In the early phases of exposure, each shock reliably triggered a somatic action potential. As this depression of excitability proceeded, however, shocks failed to produce an action potential, leaving a smaller potential deflection (fig. 9A, traces at 5 min). By 7 min, only the first of three shocks generally produced an action potential. Some neurons failed to produce responses of vagal nerve stimulation completely, while others exhibited small (< 30 mV) subthreshold depolarizations. By 9 min of ketamine perfusion in all C-type neurons tested (fig. 9B), all shocks failed to produce any measurable response in the soma. Note that as perfusion time increased, response variability across neurons increased as fewer shocks successfully elicited somatic action potentials.

Discussion

A spectrum of cranial afferents from visceral organs synapse onto mNTS neurons, and this is the first step in local integration of this information.[9,24] NTS features strong reciprocal projections with supramedullary brain regions (*e.g.*, paraventricular nucleus of the hypothalamus).[6] Nonetheless, the core pathways of many reflexes that require mNTS, such as the cardiac arterial baroreflex, operate similarly in resting intact conditions and after decerebration.[25] Thus, the basic scheme of such medullary autonomic regulation consists of mNTS neurons that then project largely within the brain stem to caudal ventrolateral medulla and nucleus ambiguus, and these pathways then connect to central sympathetic premotor neurons and peripheral parasympathetic postganglionic neurons, respectively.[6] In these reflex pathways, glutamate is the major excitatory neurotransmitter including at mNTS. Thus, for example, microinjection of glutamate receptor antagonists into the mNTS blunts baroreflex responses.[26] To understand the effects of ketamine on cardiovascular regulation, we evaluated whether mNTS synaptic transmission or neuronal excitability might represent key potential sites of action.

Integrated responses to anesthetics likely involve multiple interactions among a spectrum of effected targets, such as ligand and voltage gated ion channels and receptor mechanisms.[27] The cardiovascular system represents an interesting regulatory target for anesthetics with a distributed network of potential sites of action within the central and peripheral nervous system as well as peripheral cardiovascular effectors, such as the heart and vasculature. Peripheral cardiovascular actions of ketamine have been observed in isolated hearts[28] at greater than 100 μM or in isolated cardiac myocyte sodium and calcium currents (30–300 μM).[29] Other potential targets include NMDA receptors and synaptic transmission at spinal sympathetic preganglionics[30] and sympathetic postganglionic transmission (IC_{50} = 200 μM,[31]). Neuronal nicotinic receptors likely contribute to these alterations in ganglionic[32] as well as central autonomic[33] transmission. Early ketamine experiments on cardiovascular regulation clearly pointed to the importance of central nervous system sites of action that were linked to afferent neural inputs, such as baroreceptors. For example, the pressor response often observed during systemic delivery of ketamine was absent in an isolated heart–lung preparation, and instead, ketamine evoked cardiac depression presumably by direct end-organ actions.[34] Since decerebration did not alter the response to ketamine, the primary targets for ketamine to alter car-

Table 1. Ketamine (100 μm) Actions on Action Potential Characteristics in A-type and C-type Nodose Neurons

	Vagus Nerve Stimulation Site				Soma Stimulation Site			
	C-type (35–36°C, n = 4)		C-type (21–23°C, n = 9)		C-type (21–23°C, n = 4)		A-type (21–23°C, n = 3)	
Protocol	Control	3 min	Control	3 min	Control	3 min	Control	3 min
AP_{Peak}, mV	53.9 ± 1.9	46.8 ± 4.3	54.4 ± 5.8	45.3 ± 8.4†	52.9 ± 4.9	44.1 ± 10.7	49.5 ± 4.6	49.6 ± 4.9
AHP_{Peak}, mV	−70.4 ± 2.6	−72.4 ± 3.2	−63.8 ± 3.1	−63.7 ± 4.0	−67.0 ± 3.6	−67.5 ± 3.3	−68.1 ± 1.8	−69.3 ± 3.0
APD_{50}, ms	1.34 ± 0.10	2.9 ± 0.5†	3.04 ± 0.73	4.7 ± 1.2‡	2.95 ± 0.58	4.7 ± 1.1*	0.70 ± 0.12	0.74 ± 0.17
AHP_{80}, ms	32.5 ± 6.5	33.1 ± 12.9	25.2 ± 23.5	33.1 ± 12.9	54.3 ± 32.6	65.36 ± 33.8	21.2 ± 17.0	17.2 ± 14.1
UV_{APD50}, V/s	266.1 ± 55.8	89.8 ± 27.1†	120.8 ± 35.0	71.3 ± 40.2‡	99.0 ± 39.8	66.3 ± 25.7*	317.9 ± 33.7	323.0 ± 35.1
UV_{MAX}, V/s	400.0 ± 64.9	169.2 ± 35.6†	180.4 ± 50.6	113.2 ± 66.0‡	165.5 ± 38.4	115.0 ± 50.5†	408.0 ± 50.0	413.3 ± 59.0
DV_{APD50}, V/s	−75.7 ± 18.2	−45.8 ± 12.3†	−29.0 ± 12.5	−19.6 ± 7.2†	−26.0 ± 7.5	−14.3 ± 7.5*	−154.5 ± 66.6	−156.9 ± 81.1
DV_{MAX}, V/s	−101.6 ± 11.6	−75.8 ± 15.2*	−47.8 ± 8.8	−33.6 ± 9.3†	−46.8 ± 4.6	−28.3 ± 8.4*	−184.1 ± 63.1	−194.3 ± 78.3
CV, m/s	1.34 ± 0.05	0.79 ± 0.06†	0.73 ± 0.11	0.53 ± 0.06‡	—	—	—	—

*$P < 0.05$; †$P < 0.01$; ‡$P < 0.001$; significant difference from control.

AHP_{80} = time to dissipate 80% of the AHP; AHP_{Peak} = peak afterhyperpolarization; AP_{Peak} = action potential (AP) peak amplitude; APD_{50} = AP duration at one-half the peak-to-peak amplitude; CV = conduction velocities; DV_{APD50} = downstroke velocity as measured at the APD_{50}; DV_{MAX} = maximum downstroke velocity; UV_{APD50} = upstroke velocity as measured at the APD_{50}; UV_{MAX} = maximum upstroke velocity.

diovascular autonomic regulation may well lie within the brain stem.[4,17,18] Interestingly, elimination of baroreceptor afferent inputs by sinoaortic denervation attenuated the cardiovascular responses to ketamine, suggesting that such afferents play a role in the pressor actions of ketamine.[17,35] Bradycardic responses to activation of the peripheral cut end of the cardiac vagus nerve were unaltered by ketamine, suggesting that their peripheral function and cardiac responsiveness are preserved and that more central mechanisms are responsible for cardiac parasympathetic inhibition during ketamine.[4] Together, these studies of intact animals suggest that inhibition of afferent synaptic transmission in mNTS could be a mechanism of action of ketamine.

Activation of ST fibers evokes short-latency eEPSCs in mNTS neurons that belong to two groups—capsaicin sensitive and capsaicin resistant—that we associate with unmyelinated, C-type and myelinated, A-type afferents, respectively.[11] In cardiovascular reflex regulation, the contributions of C-type baroreceptor afferents appear to elicit stronger and longer-lasting depressor responses than A-type afferents.[12–14] Here, we found that afferent transmission to most mNTS neurons of both subtypes was mediated entirely by non-NMDA receptors[22]—an inotropic glutamate receptor well known to be resistant to ketamine.[36] However, in a small subset of capsaicin-resistant mNTS neurons, ST activation evoked eEPSCs that activated postsynaptic NMDA as well as non-NMDA receptors. The NMDA receptor response in such neurons appeared as a slow component of synaptic current that was increased in zero-Mg^{2+} conditions and blocked by the selective antagonist AP5. Low concentrations (10–100 μM) of ketamine completely blocked this low-amplitude NMDA component without significantly altering the fast, much larger non-NMDA component. Such a differential selectivity of ketamine for glutamatergic receptors is well established.[37] This difference in postsynaptic NMDA receptors may be the basis for an important action of ketamine on ST synaptic transmission that will functionally differ across capsaicin-sensitive and -resistant mNTS neuron subtypes. These results suggest that NMDA receptors may be a modulatory component in the A-type, capsaicin-resistant pathway, but the ramifications of such a preferential NMDA receptor presence are unclear. Given the association of NMDA receptors with synaptic plasticity,[38] their differential presence in mNTS may represent one mechanism differentiating these pathways that has previously not been appreciated. Together, our findings suggest a mechanism for differential sensitivity to ketamine at the first synapse of autonomic reflexes, and low concentrations of ketamine might inhibit the NMDA receptor component of excitation specifically within the A-type (capsaicin-resistant) afferent pathway through the medulla.

Surprisingly, raising ketamine concentrations further (> 100 μM) blocked ST transmission completely, first in capsaicin-sensitive neurons and then at the highest concentrations also in capsaicin-resistant neurons. Two aspects of this blockade suggested a presynaptic rather than a postsynaptic mechanism. First, autonomous sEPSCs that utilize the same non-NMDA glutamate receptor subtype were present in both capsaicin-resistant and capsaicin-sensitive mNTS neurons even at the very highest concentrations (1–3 mM) of ketamine tested. At such ketamine concentrations, ST eEPSCs were blocked in the very same neurons in which sEPSCs persisted. Those ketamine-insensitive sEPSCs were blocked by the selective non-NMDA antagonist NBQX, suggesting that the glutamate release mechanism as well as the postsynaptic non-NMDA receptors remained functional. A second clue was the very sudden onset of ST eEPSC blockade as ketamine concentration was increased. Rather than a progressive, concentration-graded decline in eEPSC amplitude as expected if compromise of postsynaptic glutamate receptor function were responsible, synaptic transmission typically failed in a nearly all-or-none man-

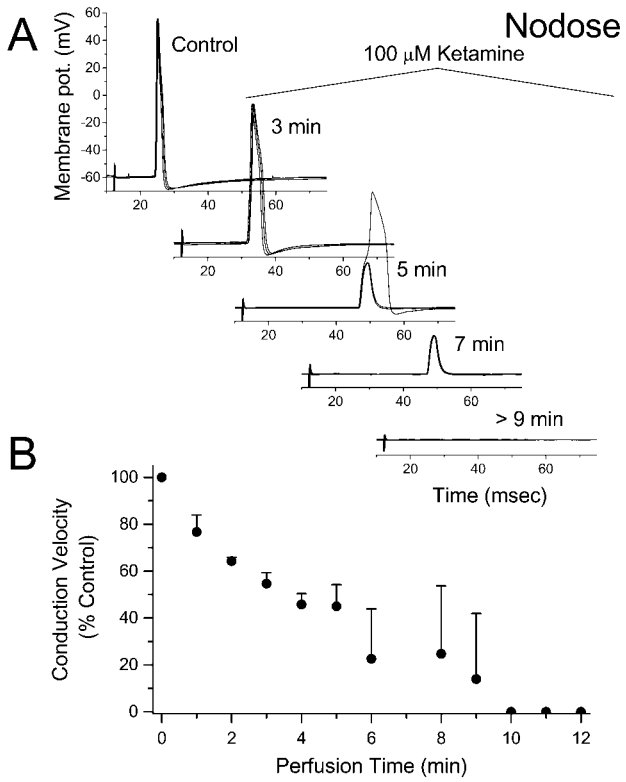

Fig. 9. Time course to conduction failure during 100-μM ketamine perfusion. A representative selection of action potential traces are displayed for the times indicated following the beginning of exposure to 100 μM ketamine at physiologic temperatures (35–36°C, *A*). This is the same neuron as presented in fig. 7A. Each frame displays responses to three consecutive vagal shocks at 1 Hz. Average conduction velocity (normalized, *B*) of C-type afferent fiber (1.4 m/s, control). Data are averages of four C-type neurons except for points at 10, 11, and 12 min, where n = 3. Note that as perfusion time increased, the response variance increased (SDs) as fewer shocks were able to elicit somatic action potentials and conduction velocity dropped to zero.

ner. Together, this profile of findings pointed to the likely involvement of presynaptic mechanisms controlling the release of glutamate from the afferent ending or ST axon. To test this concept, we studied ketamine actions on nodose ganglion neurons, the source neurons of the afferent presynaptic axons within mNTS.

The differential sensitivity to ketamine with afferent subtype is consistent with the well-known differences in the cellular properties between A- and C-type afferents, including their ion channel expression.[39–43] Certainly, comparisons of postsynaptic responses to synaptically released glutamate from ST afferents and unidentified glutamatergic endings are relatively indirect. While a number of potential mechanisms could be envisioned, the abruptness of the block in relation to concentration and the presence of increasing ST synaptic failures strongly suggested failures of presynaptic action potentials. Lower concentrations of ketamine blocked C-type action potentials than in A-type nodose neurons, and this observation supports the hypothesis that ketamine is preferentially acting at ST afferents. Lower concentrations of ketamine blocked axonal conduction measured at the vagal nerve trunk as well as somatic action potential generation in C-type neurons than in A-type neurons. We believe that these nodose properties most likely closely reflect the properties of the axons entering the brain stem to synapse on mNTS neurons as has been observed previously.[44] Therefore, the correlation between peripheral (nodose ganglion) and central (NTS slice) responses of these afferents offers a consistent view of the presynaptic element in afferent synaptic transmission.[24] NMDA receptors were activated in a specific minority of neurons (a small subgroup of capsaicin-resistant mNTS neurons), and these were much more sensitive to ketamine than the synaptic failure. Together, our findings suggest that ketamine acts presynaptically, most likely at ion channels, to block ST synaptic transmission selectively and differentially. Thus, an important corollary is that glutamate release from central neurons contacting mNTS utilizes intrinsically different ion channels that are less sensitive to ketamine than are afferent endings. Central and peripheral neurons are known to express different Na^+ channels, for example,[45] but this interaction within a single central nervous system site reinforces the notion that integrated anesthetic actions may best be appreciated in the context of the diversity of potential targets.[27] Together, our experimental results consistently show that compromise of afferent function leads to failure of C-type fibers at lower concentrations of ketamine than for A-type afferents.

Although our studies clearly identify NMDA receptors as a postsynaptic site of ketamine action, the precise presynaptic cellular targets are less clear. Ketamine may act at ion channels that are known to differ between these neuron types. For example, A- and C-type nodose neurons differ substantially in their expression of tetrodotoxin-sensitive and -resistant Na^+ currents,[39,46] and ketamine (IC_{50} = 200 μM) depresses tetrodotoxin-sensitive sodium uptake in brain.[35] Peripheral nerve axonal sodium channels are more sensitive to ketamine than voltage dependent potassium channels ($IC_{50} \approx 300$ *vs.* > 940 μM).[47] However, the inhibition of potassium channels in neuroblastoma cells by ketamine at clinical concentrations has been correlated to anesthetic actions.[48] Central nervous system and peripheral Na^+ channels are sensitive to volatile anesthetics with characteristic shifts in steady state inactivation.[49] Interestingly, tetrodotoxin-resistant Na^+ channels in the inactivated state[50] were inhibited in dorsal root ganglion neurons at similar concentrations (IC_{50} = 300 μM) to our capsaicin-sensitive eEPSCs in mNTS. In the nodose ganglion, tetrodotoxin-resistant Na^+ channel expression is limited to C-type sensory neurons.[46] Particularly intriguing and perhaps correlated are the observations that the cardiac parasympathetic preganglionic neurons in nucleus ambiguus also express tetrodotoxin-resistant Na^+ channels,[51] and these

currents are sensitive to ketamine.[52] A general aspect of ion channel effects worth considering is that conduction likely fails well before major compromise of ion currents. This was certainly the case in our nodose ketamine results in which conduction failed well before somatic action potential generation. At this point, however, there is insufficient evidence to identify any one of these potential targets as the presynaptic ketamine site(s) of action on the afferent processes.

In conclusion, our studies suggest that ketamine compromises mNTS function by multiple potential mechanisms at more than one anatomical site (presynaptic ion channels and postsynaptic NMDA receptors). Unexpectedly, the synaptic responses to ketamine in mNTS are different depending on the identity of the afferent input subtype. We have clearly identified the potential for visceral afferents and their central synaptic transmission as a major locus of action. This differential pattern of action by ketamine in these brain stem pathways is an interesting new factor and may be relevant to a variety of regulatory mechanisms based in mNTS.

References

1. Reves JG, Glass PSA, Lubarsky DA: Nonbarbiturate intravenous anesthetics, Anesthesia, 5th edition. Edited by Miller RD. New York, Churchill Livingstone, 2000, pp 228–72
2. Slogoff S, Allen GW: The role of baroreceptors in the cardiovascular response to ketamine. Anesth Analg 1974; 53:704–7
3. Akine A, Suzuka H, Hayashida Y, Kato Y: Effects of ketamine and propofol on autonomic cardiovascular function in chronically instrumented rats. Auton Neurosci 2001; 87:201–8
4. McGrath JC, MacKenzie JE, Millar RA: Effects of ketamine on central sympathetic discharge and the baroreceptor reflex during mechanical ventilation. Br J Anaesth 1975; 47:1141–7
5. White PF, Way WL, Trevor AJ: Ketamine: Its pharmacology and therapeutic uses. ANESTHESIOLOGY 1982; 56:119–36
6. Loewy AD: Central autonomic pathways, Central Regulation of Autonomic Functions. Edited by Loewy AD, Spyer KM. New York, Oxford, 1990, pp 88–103
7. Chang KSK, Lee JS, Morrow DR, Andresen MC: Intravenous ketamine inhibits cardiovascular responses to NMDA in nucleus tractus solitarius in unanesthetized decerebrate rats. Anesth Analg 2002; 94:S48
8. Ogawa A, Uemura M, Kataoka Y, Ol K, Inokuchi T: Effects of ketamine on cardiovascular responses mediated by *N*-methyl-D-aspartate receptor in the rat nucleus tractus solitarius. ANESTHESIOLOGY 1993; 78:163–7
9. Andresen MC, Kunze DL: Nucleus tractus solitarius: gateway to neural circulatory control. Annu Rev Physiol 1994; 56:93–116
10. Caterina MJ, Julius D: The vanilloid receptor: A molecular gateway to the pain pathway. Annu Rev Neurosci 2001; 24:487–517
11. Doyle MW, Bailey TW, Jin Y-H, Andresen MC: Vanilloid receptors presynaptically modulate visceral afferent synaptic transmission in nucleus tractus solitarius. J Neurosci 2002; 22:8222–9
12. Fan W, Andresen MC: Differential frequency-dependent reflex integration of myelinated and nonmyelinated rat aortic baroreceptors. Am J Physiol 1998; 275:H632–40
13. Fan W, Schild JH, Andresen MC: Graded and dynamic reflex summation of myelinated and unmyelinated rat aortic baroreceptors. Am J Physiol 1999; 277: R748–56
14. Kumada M, Terui N, Kuwaki T: Arterial baroreceptor reflex: Its central and peripheral neural mechanisms. Prog Neurobiol 1990; 35:331–61
15. Seagard JL, Gallenberg LA, Hopp FA, Dean C: Acute resetting in two functionally different types of carotid baroreceptors. Circ Res 1992; 70:559–65
16. Seagard JL, Dean C, Hopp FA: Discharge patterns of baroreceptor-modulated neurons in the nucleus tractus solitarius. Neurosci. Lett 1995; 191:13–8
17. Blake DW, Korner PI: Role of baroreceptor reflexes in the hemodynamic and heart rate responses to althesin, ketamine and thiopentone anesthesia. J Auton Nerv Syst 1981; 3:55–70
18. Blake DW, Korner PI: Effects of ketamine and althesin anesthesia on baroreceptor–heart rate reflex and hemodynamics of intact and pontine rabbits. J Auton Nerv Syst 1982; 5:145–54
19. Doyle MW, Andresen MC: Reliability of monosynaptic transmission in brain stem neurons in vitro. J Neurophysiol 2001; 85:2213–23
20. Mendelowitz D, Yang M, Andresen MC, Kunze DL: Localization and retention in vitro of fluorescently labeled aortic baroreceptor terminals on neurons from the nucleus tractus solitarius. Brain Res 1992; 581:339–43
21. Li BY, Schild JH: Patch clamp electrophysiology in the nodose ganglia of the adult rat. J Neurosci. Meth 2002; 115:157–67
22. Andresen MC, Yang M: Non-NMDA receptors mediate sensory afferent synaptic transmission in medial nucleus tractus solitarius. Am J Physiol 1990; 259:H1307–11
23. Nakagawa T, Shirasaki T, Tateishi N, Murase K, Akaike N: Effects of antagonists on *N*-methyl-D-aspartate response in acutely isolated nucleus tractus solitarii neurons of the rat. Neurosci Lett 1990; 113:169–74
24. Andresen MC, Doyle MW, Jin Y-H, Bailey TW: Cellular mechanisms of baroreceptor integration at the nucleus tractus solitarius. Ann N Y Acad Sci 2001; 940:132–41
25. Lee JS, Andresen MC, Morrow D, Chang KSK: Isoflurane depresses baroreflex control of heart rate in decerebrate rats. ANESTHESIOLOGY 2002; 96:1214–22
26. Ohta H, Talman WT: Both NMDA and non-NMDA receptors in the NTS participate in the baroreceptor reflex in rats. Am J Physiol 1994; 267:R1065–70
27. Urban BW, Friederich P: Anesthetic mechanisms in-vitro and in general anesthesia. Toxicol Lett 1998; 100–101:9–16
28. Stowe DF, Bosnjak ZJ, Kampine JP: Comparison of etomidate, ketamine, midazolam, propofol, and thiopental on function and metabolism of isolated hearts. Anesth Analg 1992; 74:547–58
29. Hara Y, Chugun A, Nakaya H, Kondo H: Tonic block of the sodium and calcium currents by ketamine in isolated guinea pig ventricular myocytes. J Vet Med Sci 1998; 60:479–83
30. Shen E, Mo N, Dun NJ: APV-sensitive dorsal root afferent transmission to neonate rat sympathetic preganglionic neurons in vitro. J Neurophysiol 1990; 64:991–9
31. Mahmoodi V, Byrne AJ, Healy TE, Hussain SZ: Effect of ketamine on transmission in sympathetic ganglia. Br J Anaesth 1980; 52:371–5
32. Tassonyi E, Charpantier E, Muller D, Dumont L, Bertrand D: The role of nicotinic acetylcholine receptors in the mechanisms of anesthesia. Brain Res Bull 2002; 57:133–50
33. Irnaten M, Wang J, Venkatesan P, Evans C, Chang KSK, Andresen MC, Mendelowitz D: Ketamine inhibits presynaptic and postsynaptic nicotinic excitation of identified cardiac parasympathetic neurons in nucleus ambiguus. ANESTHESIOLOGY 2002; 96:667–74
34. Traber DL, Wilson RD, Priano LL: Differentiation of the cardiovascular effects of CI-581. Anesth Analg 1968; 47:769–78
35. Sasao J, Taneyama C, Kohno N, Goto H: The effects of ketamine on renal sympathetic nerve activity and phrenic nerve activity in rabbits (with vagotomy) with and without afferent inputs from peripheral receptors. Anesth Analg 1996; 82:362–7
36. Wakasugi M, Hirota K, Roth SH, Ito Y: The effects of general anesthetics on excitatory and inhibitory synaptic transmission in area CA1 of the rat hippocampus *in vitro*. Anesth Analg 1999; 88:676–80
37. Reves JG, Glass PSA, Lubarsky DA: Nonbarbiturate intravenous anesthetics, Anesthesia, 5th edition. Edited by Miller RD. New York, Churchill Livingstone, 2000, pp 228–72
38. Malenka RC, Nicoll RA: NMDA-receptor-dependent synaptic plasticity: Multiple forms and mechanisms. Trends Neurosci 1993; 16:521–7
39. Schild JH, Clark JW, Hay M, Mendelowitz D, Andresen MC, Kunze DL: A- and C-type nodose sensory neurons: Model interpretations of dynamic discharge characteristics. J Neurophysiol 1994; 71:2338–58
40. Nowycky MC: Voltage-gated ion channels in dorsal root ganglion neurons, Sensory Neurons: Diversity, Development, and Plasticity. Edited by Scott SA. New York, Oxford University, 1992, pp 97–115
41. Amaya F, Decosterd I, Samad TA, Plumpton C, Tate S, Mannion RJ, Costigan M, Woolf CJ: Diversity of expression of the sensory neuron-specific TTX-resistant voltage-gated sodium ion channels SNS and SNS2. Mol Cell Neurosci 2000; 15:331–42
42. Black JA, Kocsis JD, Waxman SG: Ion channel organization of the myelinated fiber. TINS 1990; 13:48–54
43. Lawson SN: Morphological and biochemical cell types of sensory neurons, Sensory Neurons: Diversity, Development, and Plasticity. Edited by Scott SA. New York, Oxford University, 1992, pp 27–59
44. Mendelowitz D, Yang M, Reynolds PJ, Andresen MC: Heterogeneous functional expression of calcium channels at sensory and synaptic regions in nodose neurons. J Neurophysiol 1995; 73:872–5
45. Goldin AL: Diversity of mammalian voltage-gated sodium channels. Ann N Y Acad Sci 1999; 868:38–50

46. Schild JH, Kunze DL: Experimental and modeling study of Na^+ current heterogeneity in rat nodose neurons and its impact on neuronal discharge. J Neurophysiol 1997; 78:3198–209

47. Brau ME, Sander F, Vogel W, Hempelmann G: Blocking mechanisms of ketamine and its enantiomers in enzymatically demyelinated peripheral nerve as revealed by single-channel experiments. ANESTHESIOLOGY 1997; 86: 394–404

48. Friederich P, Urban BW: Interaction of intravenous anesthetics with human neuronal potassium currents in relation to clinical concentrations. ANESTHESIOLOGY 1999; 91:1853–60

49. Duch DS, Rehberg B, Vysotskaya TN: Volatile anesthetics significantly suppress central and peripheral mammalian sodium channels. Toxicol Lett 1998; 101:255–63

50. Zhou ZS, Zhao ZQ: Ketamine blockage of both tetrodotoxin (TTX)-sensitive and TTX-resistant sodium channels of rat dorsal root ganglion neurons. Brain Res Bull 2000; 52:427–33

51. Mihalevich M, Neff RA, Mendelowitz D: Voltage-gated currents in identified parasympathetic cardiac neurons in the nucleus ambiguus. Brain Res 1996; 739:258–62

52. Irnaten M, Wang J, Chang KSK, Andresen MC, Mendelowitz D: Ketamine inhibits sodium currents in identified cardiac parasympathetic neurons in nucleus ambiguus. ANESTHESIOLOGY 2002; 96:659–66